Available online at www.sciencedirect.com
ScienceDirect
Journal of Solid State Chemistry 180 (2007) 988–994
JOURNAL OF SOLID STATE CHEMISTRY
www.elsevier.com/locate/jssc

A simple method for systematically controlling ZnO crystal size and growth orientation

Rong Zhang, Lei L. Kerr*

Department of Paper and Chemical Engineering, Miami University, Oxford, OH 45056, USA

Received 26 October 2006; received in revised form 19 December 2006; accepted 26 December 2006
Available online 10 January 2007

Abstract

We present a simple, easy and reproducible method to systematically control the dimension and shape evolution of zinc oxide (ZnO) as thin film on glass substrate by chemical bath deposition (CBD). The only varying factor to control crystal transformation is the molar ratio of Cd^{2+}/Zn^{2+}, R_m, in the initial chemical solution. With the increase of R_m, ZnO crystals transformed from long-and-slim hexagonal rods to fat-and-short hexagonal pyramids, and then to twinning hexagonal dots as observed by scanning electron microscopy (SEM). Film crystallinity was characterized by X-ray diffraction (XRD). Chemical component analysis by energy dispersive spectroscopy (EDS) showed that most cadmium was present in the residual solution instead of the developed film and the precipitate at the bottom of beaker. The mechanism of the cadmium effect, with different initial concentrations, on ZnO crystal transformation was tentatively addressed. We believe that cadmium influences the chelate ligands adsorption onto $(000\bar{1})$ plane of ZnO crystals, alters the crystal growth orientation, and thus directs the transformation of the size and shape of ZnO crystals.
© 2007 Elsevier Inc. All rights reserved.

Keywords: Chemical bath deposition; Zinc oxide; Crystal structure control

1. Introduction

The properties of as-synthesized ZnO such as electrical [1–4], optical [1,5], mechanical [6], photocatalytic [7] properties strongly depend on its morphologies and structures. Thus, controlling the crystal morphologies of ZnO will greatly impact its applications in optoelectronic devices, such as blue–UV light-emitting diode [8–10], transparent transistor [11], solar cells [12,13], gas sensors [14], etc. It is essential to prepare ZnO of the desired structure and develop techniques to systematically control the size and shape of ZnO crystal.

A large number of techniques have been exploited to fabricate various crystal morphologies of ZnO films. Among these, thermal evaporation [15–18], chemical vapor deposition (CVD) [19–23], molecular beam epitaxy [24], and sputtering [25,26] require high temperature or vacuum and expensive equipments.

To reduce the cost of synthesis, solution methods have attracted increased interest and have been employed to grow nano- and micro-structured ZnO. Among all the solution methods such as electrodeposition [27,28], hydrothermal process [29–31], and chemical bath deposition (CBD) [32–41], CBD has been demonstrated to be a simple approach to develop ZnO films. CBD attracts particular interests for its potential for large-scale deposition and flexible processes. Most of the researchers were able to manufacture different shapes of ZnO [32–41] using CBD. However, the systematical control of crystal evolution remains a challenge. In addition, the mechanism for the formation of different shape of crystal is far from being fully understood. The formation of different ZnO morphologies by CBD has been obtained by adjusting additives [32,33], concentration of precursor [34], substrates and catalysts [35], post annealing [36], growth time [37], templates [38], growth temperature [39], and ionic strength [40,41].

In this paper, we present another easy method to systematically control the dimension and shape of ZnO crystal in thin film by simply adjusting the molar ratio of

*Corresponding author. Fax: +1 513 529 2201.
E-mail address: kerrll@muohio.edu (L.L. Kerr).

0022-4596/$ - see front matter © 2007 Elsevier Inc. All rights reserved.
doi:10.1016/j.jssc.2006.12.026

Cd^{2+}/Zn^{2+}, R_m. With the increase of R_m, ZnO crystals in the film become shorter and fatter, transforming from slim hexagonal rods to fat-and-short hexagonal pyramids and finally to twinning hexagonal squab dots. The mechanism of Cd effect on ZnO crystal transformation is proposed. The selection of Cd^{2+} was based on the well-known CdS deposition mechanism [46]. The Cd ions combine with ammonia and form chelate ligand of $Cd(NH_3)_6^{2+}$. The key step for ZnO formation is the zinc chelate ligand, $Zn(NH_3)_4^{2+}$, which we will discuss in the later sections. We believe that the ZnO crystal shape and morphology can be controlled because Cd ions will compete with Zn ions in the reaction with ammonia and influence the formation of $Zn(NH_3)_4^{2+}$. This method is a new contribution to the field of ZnO crystal morphology control, yet it has its own advantages as following:

(1) It is a simple and easy method. Only one controlling parameter, R_m, needs to be varied to obtain various morphologies of ZnO. It allows the systematic control of crystal growth orientation, size and shape.
(2) It is an economical low-energy process with low deposition temperature (80 °C) and does not require any post-annealing processes. This could allow the potential usage of flexible polymer substrates.
(3) It is a template free method and does not require any expensive substrates, such as Si wafer [15,17,30], GaN [29], or sapphire [23,24]. In our method, commonly used microscope slides served as substrates.

2. Experiment

2.1. Microscope glass slides pretreatment

Fisher microscope glass slides were used as substrates. A three-step pretreatment was then employed to clean and dry the slides before ZnO film growth. First, bare glass slides were boiled in deionized (DI) water for 0.5 h, then ultrasonically cleaned in acetone and alcohol solution (1:1 v:v) for 1 h, and finally dried in oven at 100 °C for 5 h. After the pretreatment, these slides were ready for the following CBD.

2.2. ZnO film deposition

Aqueous solution for ZnO thin film deposition was prepared from 50 mL of 0.2 mol/L zinc acetate dihydrate ($Zn(CH_3COO)_2 \cdot 2H_2O$, Sigma–Aldrich, 98% +) and cadmium acetate dihydrate ($Cd(CH_3COO)_2 \cdot 2H_2O$, Sigma–Aldrich, 98%) with molar ratios ($R_m = Cd^{2+}/Zn^{2+}$) of 0, 0.25, 0.5, 0.75, 1.00 and 1.25. Then, the complexing agent, ammonia hydroxide of 15–20 mL (5 mol/L) (NH_4OH) was added to the above solution to adjust the pH value to 10, which gave a colorless clear solution. Thereafter, the solution was transferred into a double-wall glass bath connected with an external circulating water bath. Temperature of the external water bath was controlled at 80 °C throughout the film growth. Pretreated glass slides were then suspended vertically in the solution for ZnO film growth. After 7 h, the glass substrates as well as the wall of the reactor were fully coated with white ZnO films, which were firm and compact. Bottom of the beaker was deposited with some white precipitate. Then, the glass substrates were withdrawn from the solution, rinsed with DI H_2O, and dried at room temperature for about 5 h. Subsequently, the as-developed ZnO thin films on the glass substrates were characterized by X-ray diffraction (XRD), scanning electron microscopy (SEM), and energy dispersive spectroscopy (EDS).

2.3. Film characterization

ZnO films crystal structures were characterized by Scintag DMS 2000, Cu$K\alpha$ radiation, $\lambda = 0.154$ nm) XRD for 2θ in the range of 20–70°. Morphology studies were carried out by Zeiss Supra 35 VP-FEG SEM with an electron beam of 3 keV. Chemical composition of ZnO films was obtained with EDAX Genesis 2000 EDS.

In addition to the characterization of thin films on glass substrates, the EDS composition analysis was also conducted on the precipitates at the bottom of the beaker and residual chemical solution after deposition. Both the precipitate and residual chemical solution were dried at 100 °C before EDS analysis.

3. Results

3.1. XRD

Fig. 1 shows the XRD patterns of the as-deposited ZnO films with different Cd^{2+}/Zn^{2+} molar ratios, R_m. XRD patterns of these samples are in agreement with the typical wurtzite structure ZnO diffraction pattern (hexagonal phase, space group $P6_3mc$, JCPDS No. 36-1451). Sharp diffraction peaks shown in Fig. 1 indicate good crystallinity of ZnO films. No characteristic peak related to Cd compounds or other impurity was observed. This result indicated that the films were composed of pure ZnO phase, which was also confirmed by EDS analysis. A relatively higher intensity ratio of (002) peak to other peak shown in Figs. 1(e)–(g) ($R_m = 0.75$, 1.00 and 1.25) indicates that the preferred orientation of the film growth in these films is along c-axis [42]. Generally, the obtained ZnO films exhibit similar characteristic XRD peaks, even though they appear different morphologies.

3.2. SEM

Morphologies of ZnO films with different R_m were studied with SEM (Fig. 2). When no cadmium acetate ($R_m = 0$) or less cadmium acetate ($R_m = 0.25$) was added to the solution, long-and-slim hexagonal rods were obtained as shown in Figs. 2(a1)–(a3) and (b1)–(b3). The

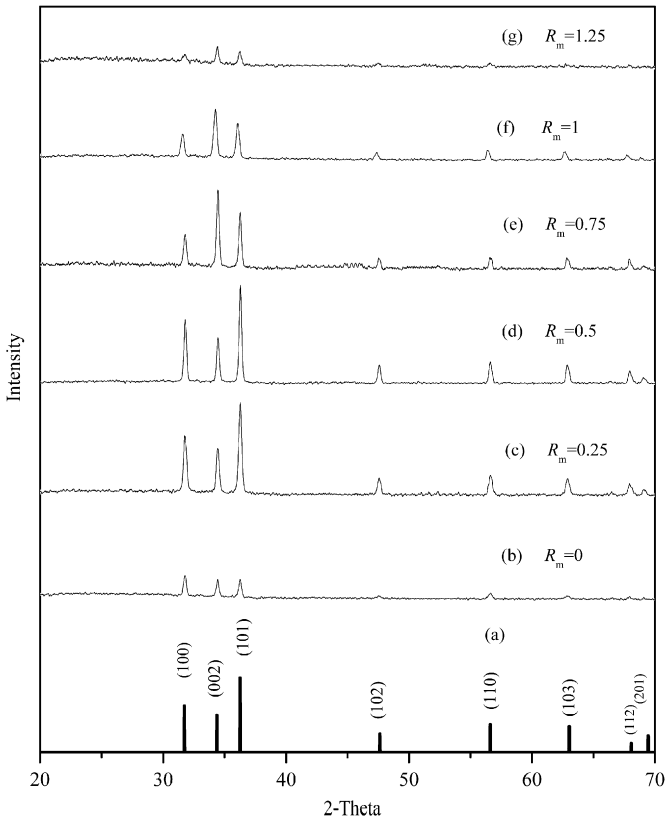

Fig. 1. XRD patterns of ZnO films with different molar ratios ($R_m = Cd^{2+}/Zn^{2+}$): (a) standard ZnO powder diffraction pattern (JCPDS No. 36-1451) (b) $R_m = 0$, long-and-slim hexagonal rods; (c) $R_m = 0.25$, long-and-slim hexagonal rod; (d) $R_m = 0.5$, fat-and-short hexagonal rods; (e) $R_m = 0.75$, fat-and-short hexagonal pyramids; (f) $R_m = 1$, fat-and-short hexagonal pyramids with the trend of twinning; (g) $R_m = 1.25$, fat-and-short twinning hexagonal dots.

average length of rods is about 10 μm, and the average diameter is around 500 nm. Continuing to increase R_m to 0.5, the shape of ZnO crystals changes from slim-and-long rods to fat-and-short hexagonal rods shown in Figs. 2(c1)–(c3). The average length is about 4 μm, while the average diameter is about 2 μm. Increasing R_m to 0.75, we have observed fat-and-short hexagonal pyramids. When R_m reaches 1, some bipyramid crystals, shown in Fig. 2(e1)–(e3), start to form. Fig. 2(e2) reveals the trend of pairing two ZnO fat-and-short hexagonal rods to form one twinning pyramid. The maximum R_m studied was 1.25, which gave ZnO crystal morphology as shown in Figs. 2(f1)–(f3). It is clearly shown that two fat-and-short hexagonal rods have been completely twinned to form one fat-and-short ZnO micro-dot. These SEM pictures showed systematical pattern of transforming ZnO crystals from long-and-slim hexagonal rods to twinning hexagonal dots.

4. Discussion on reaction mechanism

The illustration diagram (Fig. 3) showed ZnO crystal morphology evolution with the increase of Cd^{2+}/Zn^{2+} ratio, R_m. The aspect ratio, *y*-axis shown in Fig. 3, is the ratio of the average crystal diameter to the average crystal length. As we can see, the aspect ratio increases as R_m increases. ZnO crystals are transformed from slim-and-long hexagonal rods, to short-and-fat hexagonal pyramids, and finally to fat-and-short twinning hexagonal dots.

It is clear from the above results that ZnO crystal undergoes significant structure evolution with the increase of $Cd(CH_3COO)_2$ concentration in the chemical bath. To determine whether the morphology change is caused by Cd or acetate, we have done two additional experiments for the case of $R_m = 1$. In one experiment (A), cadmium acetate dihydrate was substituted with sodium acetate anhydrous (CH_3COONa, Fisher Scientific). In another experiment (B), cadmium chloride hemi(pentahydrate) ($CdCl_2 \cdot 2.5H_2O$, Sigma–Aldrich, 98%+) was used to substitute cadmium acetate dihydrate. Fig. 4(a) shows the SEM picture of the additional experiment (A). We have observed long-and-slim rods. This morphology is quiet different from the one with cadmium acetate at $R_m = 1.00$ (Figs. 2(e1)–(e3)), but similar to the one without cadmium acetate (Fig. 2(a1)–(a3)). This indicates that CH_3COO^- is not the controlling factor in ZnO crystal morphologies. Fig. 4(b) is the SEM picture of additional experiment (B). This picture showed quite similar crystal morphology to the one with cadmium acetate (Fig. 2(e1)–(e3)). Based on the observation from these two additional experiments, we can conclude that Cd^{2+} is the only key factor to control the morphologies of ZnO.

EDS analysis of deposited thin film on glass slides, precipitate at the bottom of the beaker and after-deposited solution showed that there was no cadmium in the thin films on glass slides or in the precipitate for $R_m = 0.25$, 0.5 and 0.75, and only 0.4 at% of cadmium for $R_m = 1.00$ and 1.25. EDS result also showed that most of cadmium existed in the residual solution.

To understand the reaction mechanism, the following aspects were investigated.

(1) *Why Cd exists mostly in the after-deposited solution, some amount in the precipitate and none in the thin film on glass substrate*: Ammonia, the complexing agent, in the starting deposition solution will react with Zn^{2+} and Cd^{2+} to form zinc chelate ligand [43] $Zn(NH_3)_4^{2+}$ and cadmium chelate ligand $Cd(NH_3)_6^{2+}$. The reaction constants and solubility product constants of all the possible reactions are shown in Eqs. (1)–(6).

$$Zn^{2+} + 4NH_3 \leftrightarrow Zn(NH_3)_4{}^{2+} \ (\lg \beta_{M\text{-}NH3} = 9.46)[44] \quad (1)$$

$$Zn^{2+} \text{ or } Zn(NH_3)_4{}^{2+} + 2OH^- \rightarrow Zn(OH)_2 \text{ or } Zn(OH)_2(NH_3)_4 \ (pK_{sp} = 16.92)[45] \quad (2)$$

$$Zn(OH)_2 \rightarrow ZnO + H_2O \quad (3)$$

$$Cd^{2+} + 6NH_3 \leftrightarrow Cd(NH_3)_6{}^{2+} \ (\lg \beta_{M\text{-}NH3} = 5.14)[44] \quad (4)$$

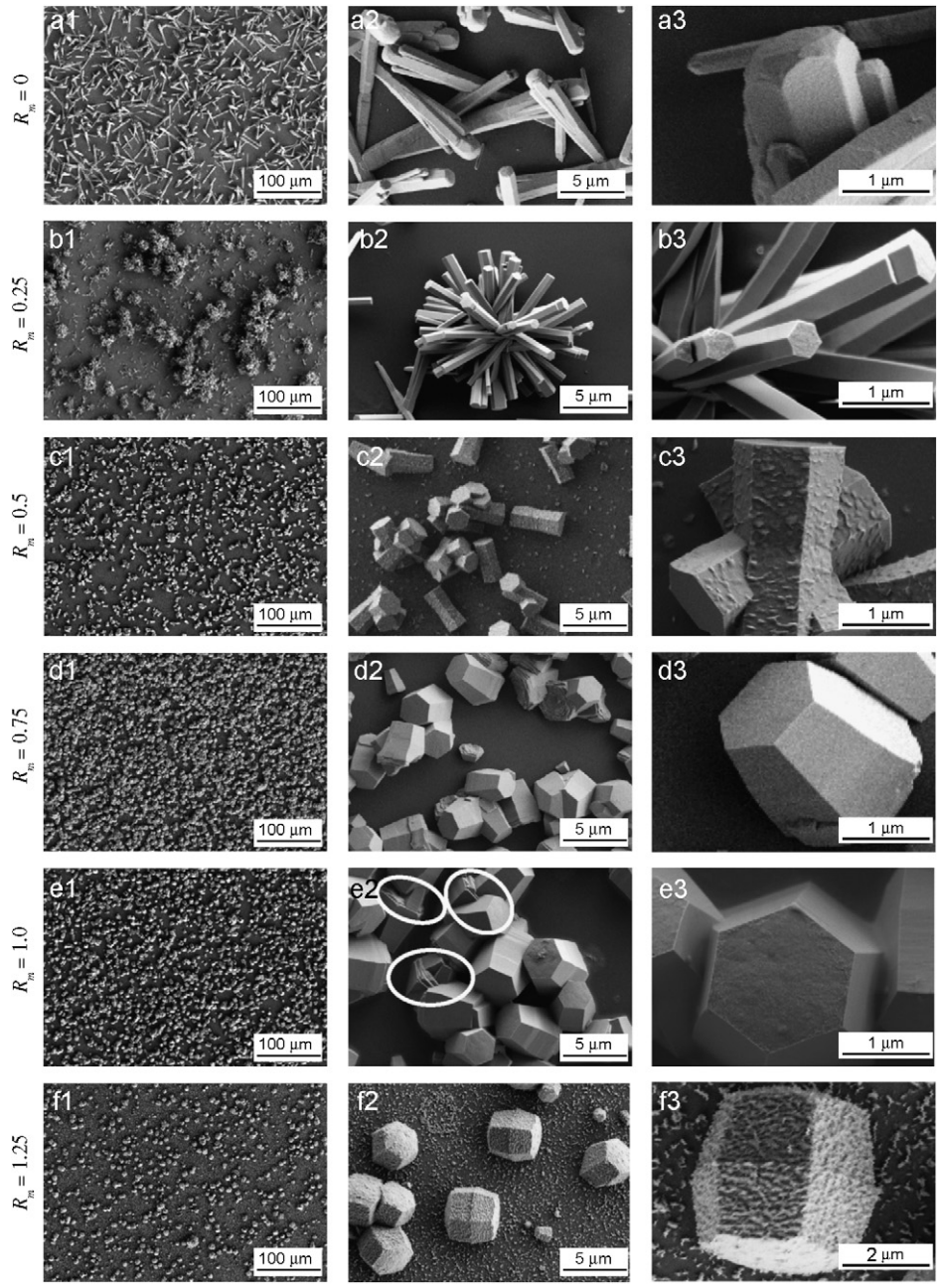

Fig. 2. SEM images of as deposited ZnO films with various morphologies: (a) $R_m = 0$, long-and-slim hexagonal rods; (b) $R_m = 0.25$, long-and-slim hexagonal rod; (c) $R_m = 0.5$, fat-and-short hexagonal rods; (d) $R_m = 0.75$, fat-and-short hexagonal pyramids; (e) $R_m = 1$, fat-and-short hexagonal pyramids with the trend of twinning; (f) $R_m = 1.25$, fat-and-short twinning hexagonal dots.

$$Cd^{2+} \text{ or } Cd(NH_3)_4{}^{2+} + 2OH^- \rightarrow Cd(OH)_2 \text{ or } Cd(OH)_2(NH_3)_4 \ (pK_{sp} = 13.6)[45] \quad (5)$$

$$NH_3 + H_2O \rightarrow NH_4{}^+ + OH^- \quad (6)$$

where lg $\beta_{M\text{-}NH3}$ = formation constant of metal ion (Zn, Cd) with NH_3, pK_{sp} = negative log of solubility product constant.

As shown in Eqs. (2) and (5), the solubility product constant of $Zn(OH)_2$ is more than three orders smaller than that of $Cd(OH)_2$. Because of this difference, Zn^{2+} or $Zn(NH_3)_4^{2+}$ won the competition in combining with OH^- in the solution to form $Zn(OH)_2$ or $Zn(OH)_2(NH_3)_4$ onto the surface of substrates, and Cd^{2+} or $Cd(NH_3)_6^{2+}$ remained in the solution. This explains the EDS result that most chemical component in the precipitate and thin films on substrate are zinc, while after-deposited solution has Cd content.

(2) *How the ZnO is formed on glass substrate*: The positive chelate ligands, $Zn(NH_3)_4^{2+}$ and $Cd(NH_3)_6^{2+}$ will form a metastable complex phase [46] with OH^-, such as $Zn(OH)_2(NH_3)_4$ (Eq. (2)), and be adsorbed onto the glass

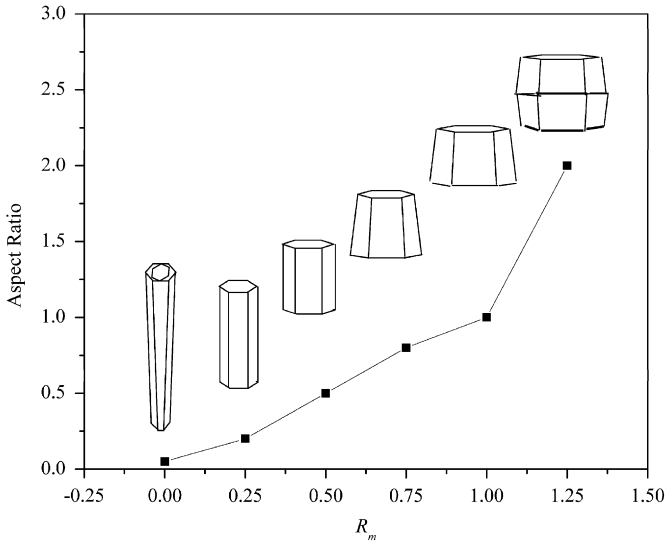

Fig. 3. Illustration of ZnO crystals morphologies evolution as a function of Cd^{2+}/Zn^{2+} molar ratio, R_m.

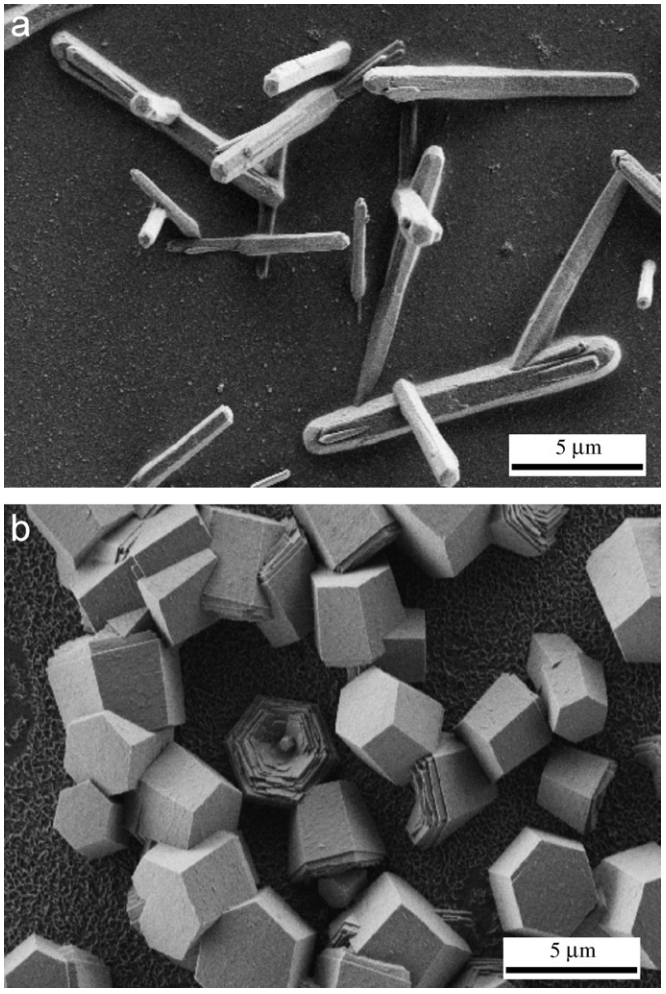

Fig. 4. SEM pictures of (a) additional experiment (A) by substituting $Cd(CH_3COO)_2$ with $Na(CH_3COO)$ at $R_m = 1$; and (b) additional experiment (B) by substituting $Cd(CH_3COO)_2$ with $CdCl_2 \cdot 2.5H_2O$ at $R_m = 1$.

substrate surface, while the free Zn^{2+} or Cd^{2+} will not be adsorbed onto the glass substrate surface. This is the key of growing thin film on substrate surface instead of forming precipitates in the solution. Due to the much smaller solubility product constant of $[Zn^{2+}][OH^-]^2$, most of the metastable complex phase will be $Zn(OH)_2(NH_3)_4$ not $Cd(OH)_2(NH_3)_4$ as indicated by Eqs. (2) and (5). This absorbed metastable complex will further decompose to form ZnO thin films (Eq. (3)). Formation of ZnO occurs at temperature as low as 50 °C [47] which is lower than the growth temperature in our case (80 °C). The as-deposited zinc oxides grown on the glass substrate surface act as nucleation centers for more ZnO crystals to grow on the substrate.

(3) *How Cd affects ZnO crystal Growth*: (a) *ZnO crystal structure and complexes adsorption*—It is well known that wurtzite ZnO crystals are mainly in the shape of hexagonal configuration. Fig. 5 describes planes of ZnO crystals from the side view (Fig. 5a) and the top view (Fig. 5b) [48]. From the microcosmic view of ZnO structure, each Zn^{2+} is surrounded by four O^{2-} stacked along *c*-axis. The positive polar plane (0001) is rich in Zn^{2+}, and the negative polar plane $(000\bar{1})$ [28,49] is rich in O^{2-}. Positive zinc and cadmium complexes, $Zn(NH_3)_4^{2+}$ and $Cd(NH_3)_6^{2+}$, are adsorbed on the negative $(000\bar{1})$ plane by electrostatic force.

(b) *ZnO growth mechanism with different Cd concentrations in the solution*: At $R_m = 0$, $Zn(NH_3)_4^{2+}$ is the only complex in the solution. The excessive NH_3 remained in the solution may prevent the amalgamation of nuclei in the initial nucleation stage [50]. Thus, individual rods in the film are the preferred crystal structure. The adsorbed $Zn(NH_3)_4^{2+}$ on $(000\bar{1})$ facet will further react with OH^- to form metastable $Zn(OH^-)_2(NH_3)_2$ to give ZnO. This reaction allows ZnO crystal growth orientation along $[000\bar{1}]$ direction as shown in the reaction mechanism model diagram (Fig. 6(a)).

While $R_m = 0.25$, cadmium complex, $Cd(NH_3)_6^{2+}$ is formed in the solution, which reduces the concentration of free NH_3. This consequently increases the mobility of nuclei and favors the aggregation of nuclei. ZnO crystals grow along $[000\bar{1}]$ direction from each nucleus to form crystal clusters congregated with hexagonal rods [34]. The Cd role has two stages. First, it reduces the free NH_3

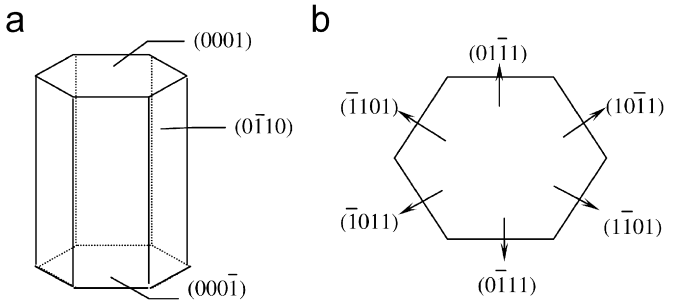

Fig. 5. Schematic diagram of ZnO crystals: (a) side view of planes; (b) top view of planes.

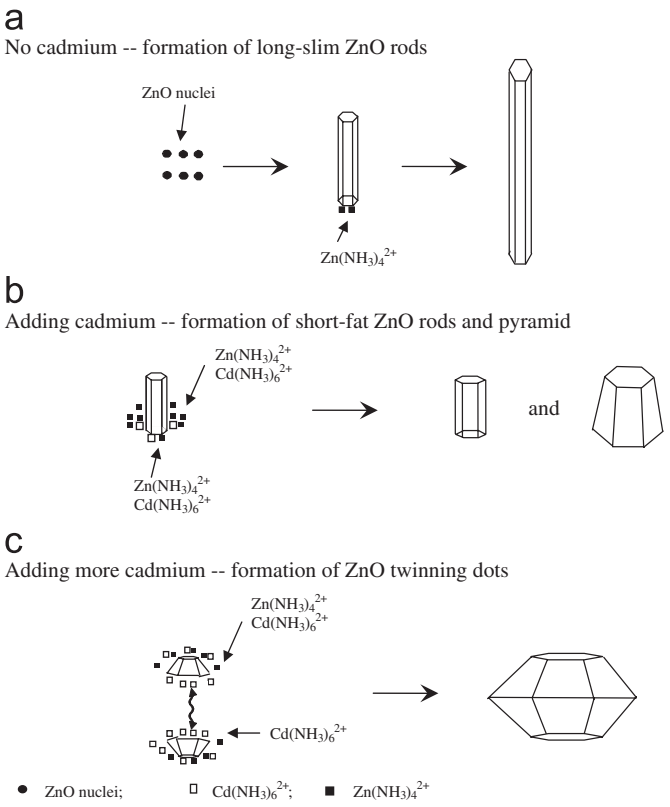

Fig. 6. Illustration of reaction mechanism for (a) formation of long-slim ZnO rods; (b) formation of short-fat ZnO rods and pyramid; (c) formation of twinning dots.

concentration to allow the formation of cluster. Then, $Cd(NH_3)_6^{2+}$ competes with $Zn(NH_3)_4^{2+}$ to be adsorbed on $(000\bar{1})$ plane and reduces the growth rate along $[000\bar{1}]$ as indicated in Fig. 6(b). Thus, we observed shorter rods at $R_m = 0.25$ than these at $R_m = 0$ in SEM pictures as presented in Fig. 2(b1)–(b3). Moreover, even though $Cd(NH_3)_4^{2+}$ was adsorbed onto $(000\bar{1})$ plane, the three-order bigger solubility product constant of $Cd(OH)_2$ than that of $Zn(OH)_2$ inhibited the formation of $Cd(OH)_2$ or CdO.

When increasing the Cd^{2+}/Zn^{2+} molar ratio R_m to 0.5, more $Cd(NH_3)_6^{2+}$ complexes are formed in the solution and compete with $Zn(NH_3)_4^{2+}$ for the adsorption sites on $(000\bar{1})$ plane. This competition inhibited adsorption of zinc complexes on $(000\bar{1})$ plane, and forced more zinc complexes to be adsorbed onto the six side planes: $(\bar{1}101)$, $(01\bar{1}1)$, $(10\bar{1}1)$, $(1\bar{1}01)$, $(0\bar{1}11)$ and $(\bar{1}011)$ as shown in Fig. 5(b). This may be the reason for the slower ZnO growth along $[000\bar{1}]$ and faster growth along the side planes, which shortens ZnO crystal length and increases its diameter to form fat-and-short pyramid rods and clusters. The XRD patterns in Fig. 1 show that the main growth direction of ZnO crystals is along (002) *c*-axis. This means that the top (0001) and the bottom $[000\bar{1}]$ planes have lower surface energies and ZnO will prefer to grow on the top and bottom planes instead of six side planes. Thus, we believe that the main competition of $Zn(NH_3)_4^{2+}$ and $Cd(NH_3)_6^{2+}$ occurs at the top (0001) and the bottom $(000\bar{1})$ planes. Further increasing R_m to 0.75, the hexagonal-pyramid-shaped ZnO rods become more obvious. This is because more cadmium complexes are formed, and more zinc complexes are pushed onto the six side planes to grow into fatter crystals. The formation mechanism of short-and-fat ZnO rods and pyramids due to the increase of cadmium content is illustrated in Fig. 6(b).

While continuing to increase R_m to 1.00, some of the pyramids started to merge together and became twinned crystals. Wang et al. reported twinned ZnO crystals formed using H_2O, weak base, KOH or NaOH [51]. Zhang et al. [52] found that poly(vinyl alcohol) (PVA) bonded growth units at (0001) plane. We designed our experiments in a way that Cd^{2+} is the only variable parameter. Therefore, it is reasonable for us to believe that the positively charged $Cd(NH_3)_6^{2+}$ bonds the negatively polarized $(000\bar{1})$ planes together and causes the twining of ZnO crystal. The formation of twins will lower the surface free energy and stabilize the crystal. Similarly, we believe that $Cd(NH_3)_6^{2+}$ in the chemical bath serves as bonding bridge to join two $(000\bar{1})$ planes as presented in Fig. 6(c). While increases R_m to 1.25, more $Cd(NH_3)_6^{2+}$ generates more twinning crystals. This explains the slightly higher cadmium content (0.4 at%) for $R_m = 1.00$ and 1.25 than that in $R_m = 0$–0.75 as revealed by EDS analysis.

In all the deposition, the time for growth is kept for 7 h. ZnO rod reaches its steady-state size after 6–7 h in our experiment. Since ammonia concentration is fixed for all experiments, as the reaction time proceeds or Cd ions are added, less base will be available to form $Zn(NH_3)_4^{2+}$. Less $Zn(NH_3)_4^{2+}$ will result in the decreased or stopped ZnO growth along *c*-axis. The focus of this work is to study the effect of Cd ions on ZnO crystal growth. Our future work will involve the investigation of reaction kinetics such as reaction time and solution concentration effects on ZnO rod length and diameter.

5. Conclusions

An easy new strategy of using cadmium to systematically control the shape and dimension evolution of ZnO crystals has been developed by CBD. By simply adjusting the concentrations of cadmium in the initial solutions, ZnO crystals have been systematically transformed from long-and-slim hexagonal rods to fat-and-short hexagonal pyramids, and then to twinning hexagonal dots. This method might offer a new opportunity for manipulating the morphologies of ZnO thin films by controlling the size and growth orientation of ZnO crystal, which has important applications in optoelectronic devices. EDS analysis verified that almost all the cadmium remained in the solution, and all the zinc existed in the thin film on glass substrate and in the precipitate. This might attribute to the three orders smaller solubility product constant of $Zn(OH)_2$ than that of $Cd(OH)_2$. The cadmium complex, $Cd(NH_3)_6^{2+}$, is believed to compete with $Zn(NH_3)_4^{2+}$ to be

adsorbed onto $(000\bar{1})$ surface of ZnO, and thus, affects the growth orientation of crystal and changes the final thin film morphology.

Acknowledgments

We would like to thank Dr. Richard E. Edelmann of Electron Microscopy Facility at Miami University for SEM and EDS operation training and for his helpful discussions on this project. We also feel grateful for the staff members of the Instrumentation Lab at Miami University for their technical support in fabricating the chemical bath reactor.

References

[1] C.X. Xu, X.W. Sun, B.J. Chen, P. Shum, S. Li, X. Hu, J. Appl. Phys. 95 (2004) 661–666.
[2] M. Wang, J. Wang, W. Chen, Y. Cui, L. Wang, Mater. Chem. Phys. 97 (2006) 219–295.
[3] X. Xing, K. Zheng, H. Xu, F. Fang, H. Shen, J. Zhang, J. Zhu, C. Ye, G. Cao, D.L. Sun, G. Chen, Micron 37 (2006) 370–373.
[4] J.P. Cheng, X.B. Zhang, X.Y. Tao, H.M. Lu, Z.Q. Luo, F. Liu, J. Phys. Chem. B 110 (2006) 10348–10353.
[5] F.–Q. He, Y.-P. Zhao, Appl. Phys. Lett. 88 (2006) 193113/1–193119/3.
[6] C.-C.M. Ma, Y.-J. Chen, H.-C. Kuan, J. Appl. Polym. Sci. 100 (2006) 508–515.
[7] F. Xu, G.-H. Du, M. Halasa, B.-L. Su, Chem. Phys. Lett. 426 (2006) 129–134.
[8] M.H. Hhuang, S. Mao, H. Feick, H. Yan, Y. Wu, H. Kind, E. Weberm, R. Russo, P. Yang, Science 292 (2001) 1897–1899.
[9] H. Cao, J.Y. Xu, D.Z. Zhang, S.-H. Chang, S.T. Ho, E.W. Seeling, X. Liu, R.P.H. Chang, Phys. Rev. Lett. 84 (2000) 5584–5587.
[10] C. Liu, J.A. Zapien, Y. Yao, X. Meng, C.S. Lee, S. Fan, Y. Lifshitz, S.T. Lee, Adv. Mater. 15 (2003) 838–841.
[11] E. Fortunato, P. Barquinha, A. Pimentel, A. Gonçalves, A. Marques, L. Pereira, R. Martins, Thin Solid Films 487 (2005) 205–211.
[12] K. Keis, E. Magnusson, H. Lindstrom, S.-E. Lindquist, A. Hagfeldt, Sol. Energy Mater. Sol. Cells 73 (2002) 51–58.
[13] J.B. Baxter, A.M. Walker, K. van Ommering, E.S. Aydil, Nanotechnology 17 (2006) S304–S312.
[14] J. Xu, Q. Pan, Y. Shun, Z. Tian, Sensors Actuators B 66 (2000) 277–279.
[15] C. Ye, X. Fang, Y. Hao, X. Teng, L. Zhang, J. Phys. Chem. B 109 (2005) 19758–19765.
[16] J. Zhang, Y. Yang, B. Xu, F. Jiang, J. Li, J. Cryst. Growth 280 (2005) 509–515.
[17] G. Shen, J.H. Cho, C.J. Lee, Chem. Phys. Lett. 401 (2005) 414–419.
[18] Y.H. Leung, A.B. Djurišić, J. Gao, M.H. Xie, W.K. Chan, Chem. Phys. Lett. 385 (2004) 155–159.
[19] S. Muthukumar, C.R. Gorla, N.W. Emanetoglu, S. Liang, Y. Lu, J. Cryst. Growth 225 (2001) 197–201.
[20] W.W. Wenas, M. Konagai, Conference Record of the 29th IEEE Photovoltaic Specialists Conference, Institute of Electrical and Electronics Engineers, 2002, p. 1130.
[21] X. Sun, H. Zhang, J. Xu, Q. Zhao, R. Wang, D. Yu, Solid State Commun. 129 (2004) 803–807.
[22] X.-Y. Zhou, H. Deng, B. Jiang, Y. Li, E.-X. Wang, Faguang Xuebao 25 (2004) 9–13.
[23] S.H. Lee, H.J. Lee, D. Oh, S.W. Lee, H. Goto, R. Buckmaster, T. Yasukawa, T. Matsue, S.-K. Hong, H.C. Ko, M.-W. Cho, T. Yao, J. Phys. Chem. B 110 (2006) 3856–3859.
[24] H. Xu, K. Ohtani, M. Yamao, H. Ohno, Phys. Status Solidi B 243 (2006) 773–777.
[25] Z.-W. Liu, J.-F. Gu, C.-W. Sun, Q.-Y. Zhang, Wuli Xuebao 55 (2006) 1965–1973.
[26] W.-Z. Lu, X.-L. Jia, X.-M. He, Rengong Jingti Xuebao 33 (2004) 35–39.
[27] B. Cao, W. Cai, H. Zeng, G. Duan, J. Appl. Phys. 99 (2006) 073516/1–073516/6.
[28] L. Xu, Y. Guo, Q. Liao, J. Zhang, D. Xu, J. Phys. Chem. B 109 (2005) 13519–13522.
[29] H.Q. Le, S.J. Chua, Y.W. Koh, K.P. Loh, E.A. Fitzgerald, J. Cryst. Growth 293 (2006) 36–42.
[30] C. Liu, Y. Masuda, Y. Wu, O. Takai, Thin Solid Films 503 (2006) 110–114.
[31] S.J. Henley, M.N.R. Ashfold, D.P. Nicholls, P. Wheatley, D. Cherns, Appl. Phys. A: Mater. Sci. Process. 79 (2004) 1169–1173.
[32] P. Lipowsky, S. Jia, R.C. Hoffmann, N.Y. Jin-Phillipp, J. Bill, M. Rühle, Int. J. Mater. Res. 97 (2006) 607–613.
[33] Z.R. Tian, J.A. Voigt, J. Liu, B. Mckenzie, M.J. Mcdermott, M.A. Rodriguez, H. Konishi, H. Xu, Nat. Mater. 2 (2003) 821–826.
[34] W. Peng, S. Qu, G. Cong, Z. Wang, Cryst. Growth Des. 6 (2006) 1518–1522.
[35] J.-Y. Lee, D. Yin, S. Horiuchi, Chem. Mater. 17 (2005) 5498–5503.
[36] J. Ouerfelli, M. Regragui, M. Morsli, G. Djeteli, K. Jondo, C. Amory, G. Tchangbedji, K. Napo, J.C. Bernède, J. Phys. D: Appl. Phys. 39 (2006) 1954–1959.
[37] Q. Li, V. Kumar, Y. Li, H. Zhang, T.J. Marks, R.P.H. Chang, Chem. Mater. 17 (2005) 1001–1006.
[38] K. Kakiuchi, E. Hosono, T. Kimura, H. Imai, S. Fujihara, J. Sol–Gel Sci. Technol. 39 (2006) 63–72.
[39] S. Hirano, K. Masuya, M. Kuwabara, J. Phys. Chem. B 108 (2004) 4576–4578.
[40] X. Liu, Z. Jin, S. Bu, J. Zhao Z. Liu, J. Am. Ceram. Soc. 89 (2006) 1226–1231.
[41] K. Govender, D.S. Boyle, P.B. Kenway, P. O'Brien, J. Mater. Chem. 14 (2004) 2575–2591.
[42] P.-A. Hu, Y.-Q. Liu, L. Fu, X.-B. Wang, D.-B. Zhu, Appl. Phys. A: Mater. Sci. Process. 78 (2004) 15–19.
[43] L. Dileo, D. Romano, L. Schaeffer, B. Gersten, C. Foster, M.C. Gelabert, J. Cryst. Growth 271 (2004) 65–73.
[44] M. Zou, H. Xu, G. Yu, Analytical Chemistry, Jilin University, Jilin, 1995, p. 352.
[45] J.A. Dean, Analytical Chemistry Handbook, McGraw-Hill, New York, 1995, p. 3.3.
[46] M. Kostoglou, N. Andritsos, A.J. Karabelas, Thin Solid Films 387 (2001) 115–117.
[47] M. Ortega-López, A. Avila-García, M.L. Albor-Aguilera, V.M. Sánchez Resendiz, Mater. Res. Bull. 38 (2003) 1241–1248.
[48] J. Joo, S.G. Kwon, J.H. Yu, T. Hyeon, Adv. Mater. 17 (2005) 1873–1877.
[49] P. Li, Y. Wei, H. Liu, X.-K. Wang, J. Solid State Chem. 178 (2005) 855–860.
[50] J. Zhang, L. Sun, J. Yin, H. Su, C. Liao, C. Yan, Chem. Mater. 14 (2002) 4172–4177.
[51] B.G. Wang, E.W. Shi, W.Z. Zhong, Cryst. Res. Technol. 33 (1998) 937–941.
[52] H. Zhang, D. Yang, D. Li, X. Ma, S. Li, D. Que, Cryst. Growth Des. 5 (2005) 547–550.